Journal Pre-proof

Phenylthiazoles with nitrogenous side chain: An approach to overcome molecular obesity

Mohamed M. Elsebaei, Nader S. Abutaleb, Abdulrahman A. Mahgoub, Daoyi Li, Mohamed Hagras, Haroon Mohammad, Mohamed N. Seleem, Abdelrahman S. Mayhoub

PII: S0223-5234(19)30727-5

DOI: https://doi.org/10.1016/j.ejmech.2019.111593

Reference: EJMECH 111593

To appear in: *European Journal of Medicinal Chemistry*

Received Date: 30 May 2019

Revised Date: 11 July 2019

Accepted Date: 5 August 2019

Please cite this article as: M.M. Elsebaei, N.S. Abutaleb, A.A. Mahgoub, D. Li, M. Hagras, H. Mohammad, M.N. Seleem, A.S. Mayhoub, Phenylthiazoles with nitrogenous side chain: An approach to overcome molecular obesity, *European Journal of Medicinal Chemistry* (2019), doi: https://doi.org/10.1016/j.ejmech.2019.111593.

This is a PDF file of an article that has undergone enhancements after acceptance, such as the addition of a cover page and metadata, and formatting for readability, but it is not yet the definitive version of record. This version will undergo additional copyediting, typesetting and review before it is published in its final form, but we are providing this version to give early visibility of the article. Please note that, during the production process, errors may be discovered which could affect the content, and all legal disclaimers that apply to the journal pertain.

© 2019 Published by Elsevier Masson SAS.

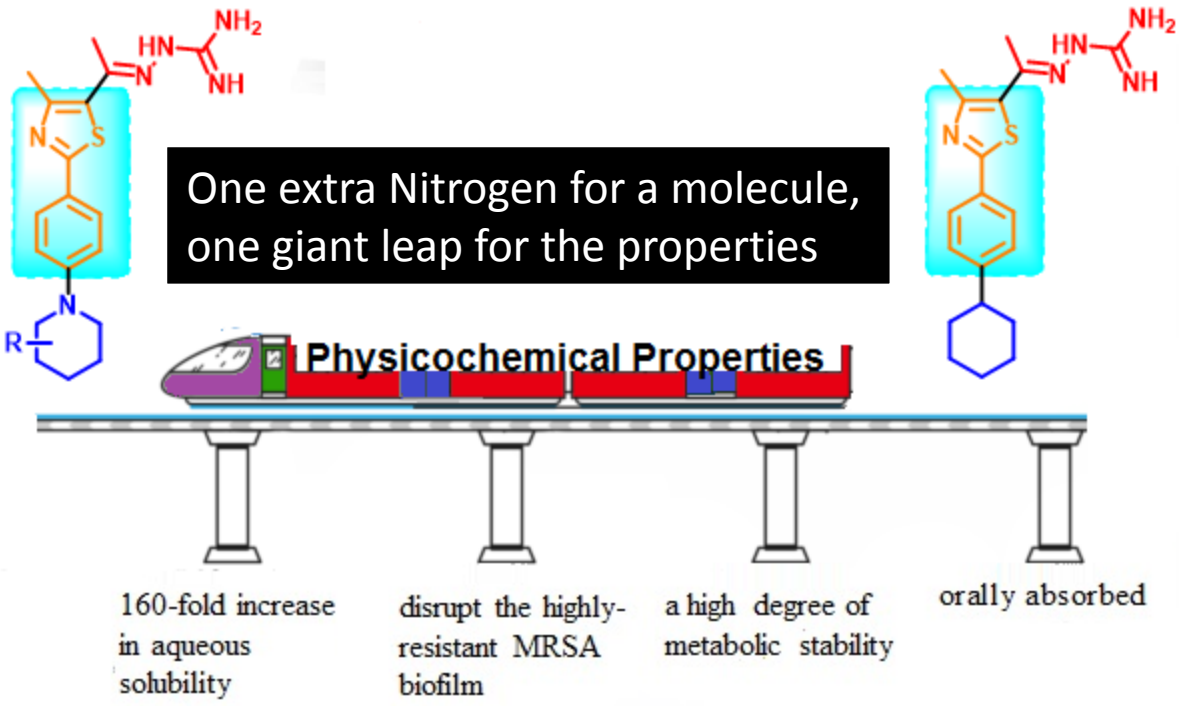

Journal Pre-proof

Journal Pre-proof

Phenylthiazoles with Nitrogenous Side Chain: An Approach to Overcome Molecular Obesity

Mohamed M. Elsebaei[a], Nader S. Abutaleb[b] , Abdulrahman A. Mahgoub[a], Daoyi Li[b], Mohamed Hagras[a], Haroon Mohammad[b], Mohamed N. Seleem[b,c**] and Abdelrahman S. Mayhoub[a,d*]

[a.] Department of Pharmaceutical Organic Chemistry, College of Pharmacy, Al-Azhar University, Cairo 11884, Egypt.

[b.] Department of Comparative Pathobiology, College of Veterinary Medicine, Purdue University, West Lafayette, IN 47907, USA.

[c.] Purdue Institute of Inflammation, Immunology, and Infectious Disease, West Lafayette, IN 47907, USA.

[d.] University of Science and Technology, Nanoscience Program, Zewail City of Science and Technology, October Gardens, 6th of October, Giza 12578, Egypt.

Corresponding Authors

** MNS; email, mseleem@purdue.edu

* ASM; e-mail, amayhoub@azhar.edu.eg

[‖]These two authors contributed equally

Journal Pre-proof

Journal Pre-proof

Abbreviations. CFU, colony forming units; CL, clearance rate; C_{max}, maximum plasma concentration; DME, dimethoxyethane; MIC, minimum inhibitory concentration; MBC, minimum bactericidal concentration; MRSA, methicillin-resistant *Staphylococcus aureus*; PK, pharmacokinetics; $t_{1/2}$, half-life; V_d, volume of distribution; T_{max}, time required to reach the maximum plasma concentration.

Journal Pre-proof

Journal Pre-proof

Abstract. A novel series of phenylthiazoles bearing cyclic amines at the phenyl-4 position was prepared with the objective of decreasing lipophilicity and improving the overall physicochemical properties and pharmacokinetic profile of the compounds. Briefly, the piperidine ring (compounds **10** and **12**) provided the best ring size in terms of antibacterial activity when tested against 16 multidrug-resistant clinical isolates. Both compounds were superior to vancomycin in the ability to eliminate methicillin-resistant *Staphylococcus aureus* (MRSA), residing within infected macrophages and to disrupt mature MRSA biofilm. Additionally, compounds **10** and **12** exhibited a fast-bactericidal mode of action *in vitro*. Furthermore, the new derivatives were 160-times more soluble in water than the previous lead compound **1b**. Consequently, compound **10** was orally bioavailable with a highly-acceptable pharmacokinetic profile *in vivo* that exhibited a half-life of 4 hours and achieved a maximum plasma concentration that exceeded the minimum inhibitory concentration (MIC) values against all tested bacterial isolates.

Journal Pre-proof

Journal Pre-proof

1. Introduction

Our group launched a project in 2014 that aimed to discover and develop a new chemical scaffold to develop a novel series of compounds with antibacterial activity against multidrug-resistant bacteria. In the past five years, more than 500 arylthiazole derivatives have been synthesized and their antibacterial profiles were thoroughly investigated.[1-14] The compounds exhibited potent antibacterial activity against pertinent Gram-positive bacterial pathogens of clinical interest including methicillin-resistant *S. aureus*, drug-resistant *Streptococcus pneumoniae*, and vancomycin-resistant enterococci (VRE) but were inactive against Gram-negative bacteria. MRSA, *S. pneumoniae*, and VRE are responsible for an array of non-invasive and systemic bacterial infections that are often resistant to treatment by more than one antibiotic. Altogether, these three bacterial pathogens have been linked to more than one million antibiotic-resistant infections and nearly 20,000 deaths annually in the United States of America alone[15]. Using transposon mutagenesis study followed by biochemical assays, it was proved that undecaprenyl diphosphate phosphatase (UppP) is the main bacterial target for our phenylthiazole antibacterial agents.[16]

Initial inspection of the structure-activity-relationships (SAR) of the arylthiazole compounds led us to cyclize the terminal *n*-butyl moiety in order to improve the lead compound's antibacterial potency [9]. However, as the antibacterial activity of the compound's improved, the modifications incorporated resulted in deterioration of the physicochemical properties and pharmacokinetic profile of the new analogs (Figure 1). In brief, cyclization of the *n*-butyl side chain of the initial lead compound **1a** lowered the MIC value against several MDR-staphylococcal strains by a factor of 5 [9]. Simultaneously, the tremendous increase in lipophilicity, as indicated by the clogP value, lowered the aqueous solubility limit from 65

μg/mL, for **1a**, to around 3 μg/mL, for **1b**. A direct consequence of this decrease in solubility was difficulty in developing a suitable formulation for **1b** to administer either orally or parenterally.

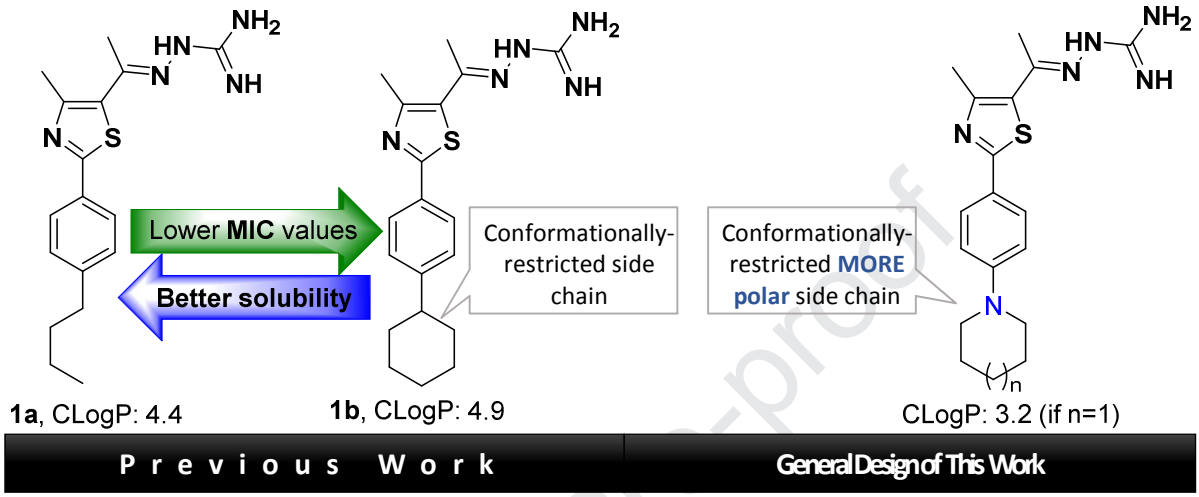

Figure 1. Overview of the aim of the present work.

Advances in formulation technology (such as hot melt extrusion [17, 18] and spray-drying [19]) can aid in solubilizing obese molecules to permit their absorption into systemic circulation. However, these advanced methods hinder excretion of obese molecules from the human body as metabolic enzymes must work aggressively to increase the polarity of these obese xenobiotics, in order to excrete them [20]. In addition to reduced aqueous solubility, compounds exhibiting a logP value above 3.5 are usually associated with increased off-target side effects [21]. Therefore, we hypothesized that decreasing the lipophilic capacity of the phenylthiazole compounds would reduce off-target effects and eventually improve the compounds' aqueous solubility and overall pharmacokinetic profile. To address this point, the cyclohexyl group in the lead compound **1b** was replaced with a cyclic amine, as depicted in Figure 1, and the analogs synthesized were evaluated for their antibacterial activity, improvement in aqueous solubility, and in vivo pharmacokinetic profile.

Scheme 1

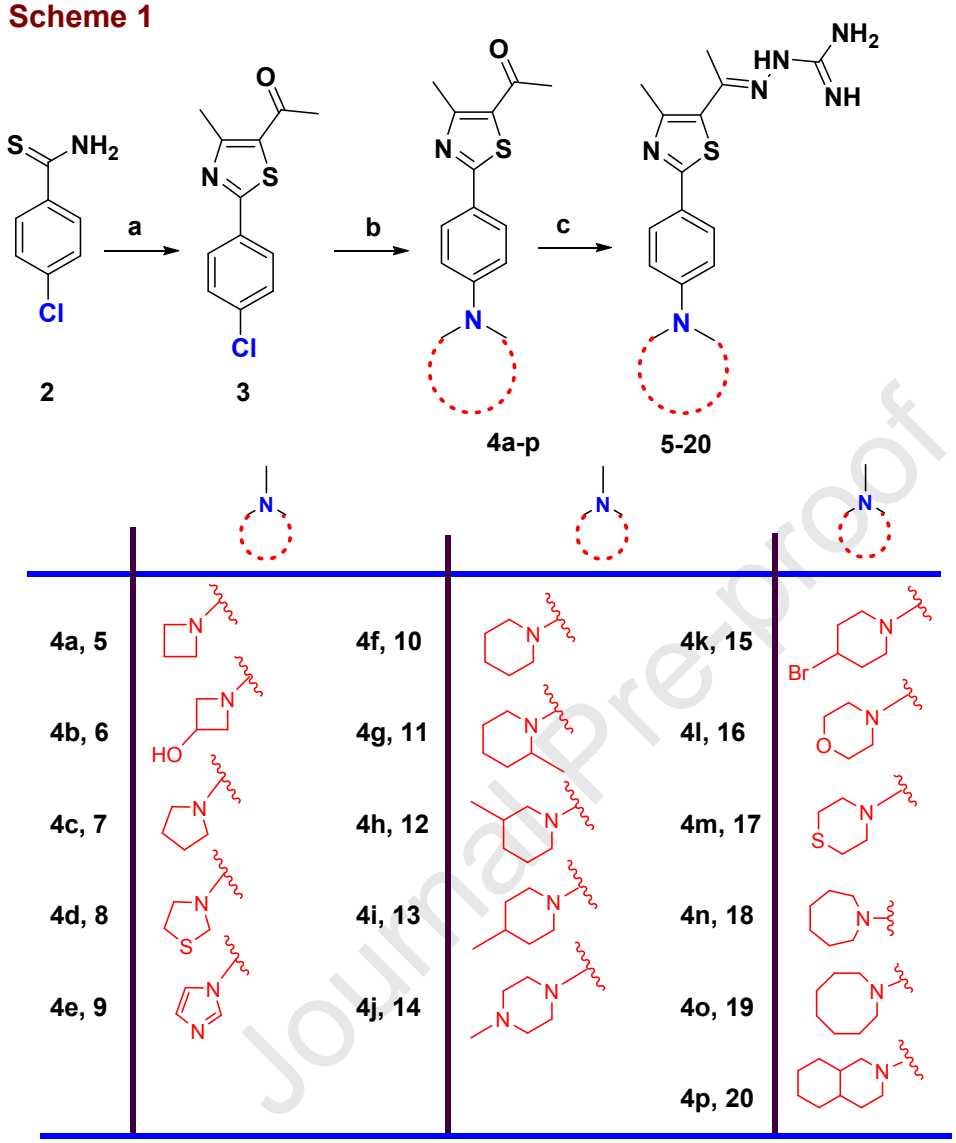

Reagents and conditions: (a) Absolute EtOH, 3-chloro-2,4-pentandion, heat to reflux, 6 h, (b) $Pd(OAc)_2$ (5% mol), X-phos (10% mol), KOtBu (2.5 equiv.), appropriate *sec*-amine, DME, heat at 200°C for 3 h; (c) aminoguanidine HCl, EtOH, conc. HCl, heat to reflux, 3 h.

2. Results and Discussion

2.1. Chemistry. Treatment of *para*-chlorobenzothioamide (**2**) with α-chloroacetylacetone yielded the key starting compound **3**, as reported previously.[22] The corresponding *sec*-amine derivatives **4a-p** were obtained using the Buchwald synthetic protocol (scheme **1**). In the first thrust, we used Cu-catalyzed C-N cross coupling protocol; i.e., copper(I) iodide and L-proline,

but the isolated yield was terribly low (< 5%). So that, we switched to the Pd-catalyzed protocol, in which Pd(II) and X-Phos ligand in a polar aprotic solvent provided the best yields of compounds **4a-p** (Scheme 1). Condensation of **4a-p** with aminoguanidine hydrochloride yielded the final products **5-20** (Scheme 1).

2.2. Biological Results and Discussion.

2.2.1. Antibacterial activity of new analogs against MRSA. The newly synthesized analogs were initially screened against the highly-pathogenic strain, MRSA USA300 [23-25]. The 6-membered piperidine side chain (compound **10**) represented the best ring size as it afforded the most potent analog from this series (MIC value of 4 μg/mL) (Table 1), which means that the target protein cannot accommodate, at this particular position, for more than 6-membered ring. The SAR appears straightforward as it pertains to the ring size. Briefly, shrinking the nitrogenous side chain gradually impaired the compounds' anti-MRSA activity as the MIC value increased to 16 μg/mL 4-times for the pyrrolidine-containing derivative **7** and was completely nullified for the azetidine-containing analog **5**. Similarly, expanding the nitrogenous ring size provided the hexamethyleneimine- and heptamethyleneimine-containing derivatives **18** and **19** with MIC values ≥ 128 μg/mL (Table 1). This observation confirms our previous hypothesis that the active site of the targeted receptor cannot accommodate rings larger than 6-membered ones.

Further attempts to increase the polarity of the side chain by using the more polar nitrogenous rings morpholine and piperazine resulted in less active derivatives (compounds **14** and **16**). Substitution with methyl groups yielded the methylpiperidines **11-13** with high variability in MIC values in which the 2-methyl and 4-methylpiperidine-containing derivatives **11** and **13** were 2 to 4-times less active than the unsubstituted piperidine **10** (Table 1). On the other hand, the 3-methyl substitution (compound **12**) maintained the same anti-MRSA inhibitory

potency as compound **10**. The MIC for the control antibiotics linezolid and vancomycin against MRSA USA300 was 1 µg/mL.

Table 1. Initial screening of the newly synthesized arylthiazole analogs against methicillin-resistant *Staphylococcus aureus* NRS384 (MRSA USA300).

Compounds/ Control Antibiotics	Side chain	MIC (µg/mL)	Compounds/ Control Antibiotics	Side chain	MIC (µg/mL)
5		>128	**14**	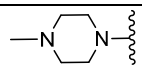	64
6	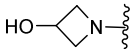	64	**15**	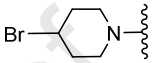	8
7	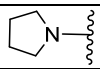	16	**16**	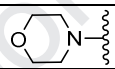	>128
8	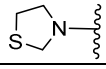	>128	**17**	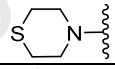	32
9	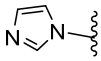	16	**18**		>128
10		4	**19**	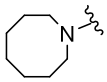	128
11	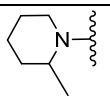	8	**20**	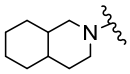	>128
12	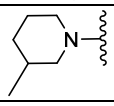	4	Linezolid	_	1
13	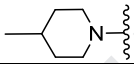	16	Vancomycin	_	1

2.2.2. Preliminary toxicological and pharmacokinetic evaluation. The most promising compounds, **10** and **12**, were tested to evaluate our hypothesis that the substitution of the cyclohexyl moiety in **1b** with cyclic amines would positively impact the physicochemical properties and PK behavior of the compounds. Before advancing to an *in vivo* PK study, compounds **10** and **12** were assessed for toxicity to mammalian cells, and both compounds exhibited a good safety profile against human colorectal cells (Caco-2) and human keratinocytes (HaCaT) (Figure 2, Panel A). Compound **12** was non-toxic to Caco-2 cells up to 32 µg/mL. This concentration is 8-times higher than the compound's corresponding MIC value against MRSA USA300. Compound **10** was non-toxic to Caco-2 cells up to 64 µg/mL, which is 16-times higher

than the compound's MIC against MRSA USA300. Similar results were observed when the compounds were tested against human keratinocytes (HaCaT) (Figure 2, Panel B).

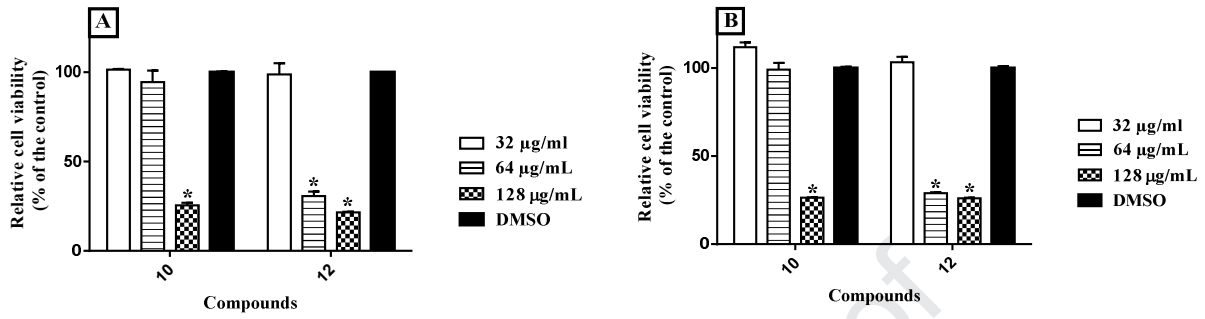

Figure 2. Toxicity analysis of compounds 10 and 12 (tested in triplicate at 32, 64 and 128 µg/mL) against A) human colorectal (Caco-2, panel A) and B) human keratinocytes (HaCaT, panel B) using the MTS 3-(4,5-dimethylthiazol-2-yl)-5-(3-carboxymethoxyphenyl)-2-(4-sulfophenyl)-2*H*-tetrazolium) assay. Results are presented as percent viable cells relative to DMSO (negative control to determine a baseline measure for the cytotoxic impact of each compound). The absorbance values represent an average of three samples analyzed for each compound. Error bars represent sample standard deviation values. The data were analyzed via two-way ANOVA with post-hoc Dunnett's test for multiple comparisons ($P<0.05$).

Physicochemical properties of candidate antibacterial agents are critical to evaluate early in drug development [26, 27]. Promising compounds with potent *in vitro* activity against a target pathogen may fail in clinical trials due to poor aqueous solubility and permeability. Thus, after confirming compounds **10** and **12** possessed good antibacterial activity and to safety to mammalian cells, we investigated the compounds' aqueous solubility profile. Both compounds exhibited a more than 160-fold increase in aqueous solubility relative to the first-generation lead compound **1b** (Table 2). The notable improvement observed supports the first part of our hypothesis that the new chemical modification, presented here, on the phenylthiazole scaffold would positively impact the compounds' physicochemical properties. Next, we tested the second part of our hypothesis, investigating the impact of incorporating the piperidine ring as part of the lipophilic side chain, on the compound's PK profile. In this vein, a PK study in rats was

performed to assess the distribution of compound **10** in the bloodstream after oral administration. Compound **10** was selected for *in vivo* PK evaluation due to its superior aqueous solubility and safety profile. The PK curve (Figure 3) of compound **10** demonstrated it reached a maximum plasma concentration (C_{max}) of 10 µg/mL (2.5 × MIC vs. MRSA USA300) ~90 minutes after administration with a biological half-life of 4 hours. Moreover, the plasma concentration of compound **10** remained above the MIC value for MRSA USA300 for nearly 7 hours. This represents a marked improvement relative to the first-generation phenylthiazoles which were metabolically unstable resulting in short half-lives and rapid hepatic clearance.[9] The PK study suggests that the piperidine-containing derivative **10** is suitable for oral administration.

Table 2. Evaluation of aqueous solubility limit of compounds **1a**, **1b**, **10** and **12** in phosphate-buffered saline (PBS).

Compounds	Solubility limit[1] (µM)
1a	65
1b	2.7
10	480
12	435

[1]Solubility limit corresponds to the highest concentration of test compound where no precipitate was detected (OD_{540}).

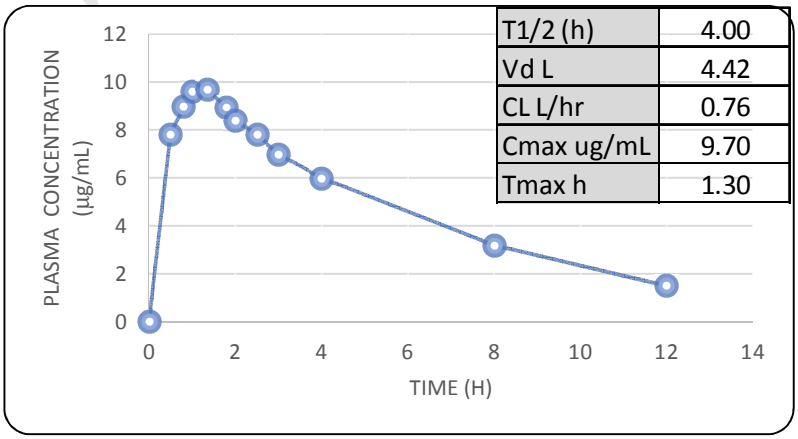

Figure 3. The pharmacokinetic profile of compound 10 after oral administration of a single dose of 50 mg/Kg in rat.

Journal Pre-proof

2.2.3. Comprehensive antibacterial profiling of compounds 10 and 12. After confirming our hypothesis that piperidine-containing phenylthiazoles (represented by compounds **10** and **12**) exhibit a markedly improved physicochemical profile compared to previously-synthesized analogs, we assessed the antibacterial profile of compounds **10** and **12** against a panel of multidrug-resistant staphylococcal isolates. Both compounds inhibited growth of the tested strains at concentrations ranging from 4 to 8 μg/mL and exhibited bactericidal activity (as the MBC values were equal to or one-fold higher than the MIC values) (Table 1S). Furthermore, the two compounds maintained the same potent bactericidal activity against other clinically-relevant Gram-positive bacterial species including vancomycin-resistant enterococci (VRE), multidrug-resistant *Streptococcus pneumoniae* and *Listeria monocytogenes* (Table 2S).

In order to confirm this bactericidal mode of action against MRSA, a time-kill assay was utilized. The new series of phenylthiazoles was superior to vancomycin in terms of the time required to exert bactericidal activity *in vitro*. Vancomycin reduced the burden of MRSA by 3-$\log_{10}$ within 12 hours and required 24 hours to reduce the burden of MRSA below the limit of detection (Figure 4). In contrast, the piperidine-containing phenylthiazoles **10** and **12** required only 4 hours to reduce the burden of MRSA below the limit of detection (Figure 4). It has been postulated that the slow bactericidal effect of antibiotics such as vancomycin can result in difficulty in clearing a bacterial infection [28, 29]. Thus, agents such as compounds **10** and **12** that can rapidly kill MRSA are highly desirable

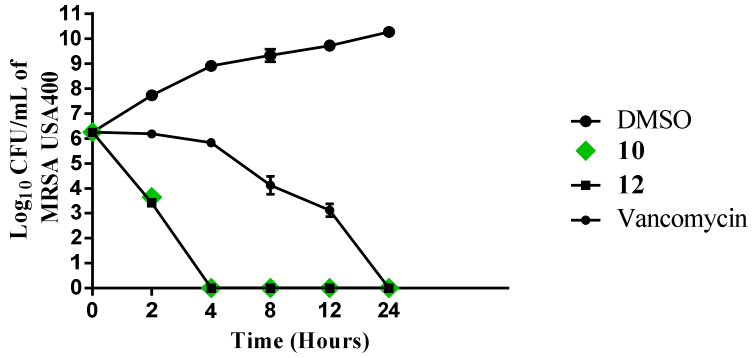

Figure 4. Killing kinetics of compounds 10 and 12 and vancomycin (tested in triplicate at 5 × MIC) against methicillin-resistant *Staphylococcus aureus* (MRSA USA400) over a 24-hour incubation period at 37 °C. DMSO (solvent for the compounds) served as a negative control. The error bars represent standard deviation values obtained from triplicate samples used for each compound/antibiotic studied.

The rapid, potent bactericidal activity of compounds **10** and **12** propelled us to investigate if these compounds could gain entry inside macrophages infected with *S. aureus* to reduce the burden of bacteria. The success of *S. aureus* as a highly-pathogenic microorganism is not only attributed to extensive release of different virulence factors but to its ability to evade host innate immune responses as well. Virulence factors released by *S. aureus* are capable of interfering with leukocyte recruitment and inhibiting production of complement factors and antimicrobial peptides [30-32]. Furthermore, *S. aureus* produces toxins, like leukocidin A/B, that are able to specifically target and kill phagocytes [33, 34]. Additionally, it has been reported that intracellular MRSA can replicate within the phagolysosome after phagocytosis by macrophages thus permitting the organism to survive and re-infect the host [35]. Most antibiotics are unable to target intracellular bacteria due to: 1) low levels of intracellular accumulation as in the case of linezolid, β-lactams, and gentamicin; 2) inactivation/loss of activity due to the acidic pH within macrophages, as with aminoglycosides; and 3) binding to lysosomal contents, as in the case of oritavancin [36, 37]. Like most antibiotics, vancomycin, the drug of last resort for treatment of

MRSA infections fails to gain entry inside infected macrophages and must be used at high concentrations to achieve significant activity against intracellular *S. aureus* [38, 39]. The previously reported intracellular clearance activity of some compounds in our series of phenylthiazole antibiotics[1, 3] encouraged us to investigate the ability of the newly-synthesized compounds to reduce the burden of intracellular MRSA present within macrophages. Compound **10** was selected for this experiment based on its superior safety profile to the murine macrophages used for the intracellular infection experiment (Figure 5A). As depicted in Figure 5, after 24 hours incubation, phenylthiazole **10** (at 2 × MIC) generated a 1.18-$\log_{10}$ reduction (equivalent to 93.2% reduction) of intracellular MRSA. This was superior to vancomycin which was unable to reduce the burden of intracellular MRSA. This result indicates that in addition to compound **10** exhibiting more rapid bactericidal activity against MRSA *in vitro* compared to vancomycin, the compound possesses an additional advantage over vancomycin in the ability to reduce the burden of intracellular MRSA within infected macrophages.

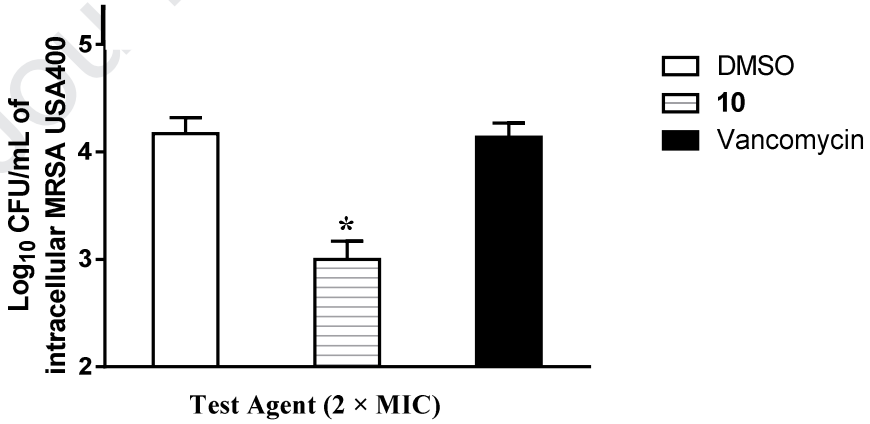

Figure 5. Effect of compound 10 and vancomycin to reduce intracellular MRSA present inside murine macrophages (J774). Data are presented as $\log_{10}$ colony forming units of MRSA USA400 per mL inside infected murine macrophages after treatment with 2×MIC of either compound **10** or vancomycin (tested in quadruplicates) for 24-hours. Data were analyzed via one-way ANOVA, with post hoc Dunnet's test for multiple comparisons ($P < 0.05$), utilizing GraphPad Prism 6.0 (GraphPad Software, La Jolla, CA). The asterisk (*) represents a significant difference between the treatment of J774 cells with compound **10** in comparison to vancomycin.

Journal Pre-proof

2.2.4. Evaluation of the anti-biofilm activity of compounds 10 and 12. Targeting factors that contribute to bacterial virulence and colonization of host tissues represents an alternative approach currently being pursued to counter the emergence of bacterial resistance to antibiotics [40]. One example of this is the identification and development of molecules capable of inhibiting or eradicating bacterial biofilms [41]. Biofilms can form on the surfaces of indwelling catheters and implanted medical devices [42, 43]. These biofilms can lead to fatal bloodstream infections which are associated with substantial treatment costs [44]. Many invasive infections caused by *S. aureus* develop from bacterial biofilms formed on the surface of implanted medical devices [42, 45]. This problem could be further exacerbated as bacteria embedded within biofilms exhibit increased resistance to antibiotics [3, 46]. Surgical intervention through physical replacement of the infected medical implant is the primary option currently available to cliniciansbut is assoictaed with multiple risks and complications [47]. Identifying molecules capable of disrupting adherent biofilm from these devices would provide a suitable alternative to surgical intervention. Previous reports have demosntrated that phenylthiazoles are able to disrupt pre-formed bacterial biofilms [3, 5, 8, 48]. Thus compounds **10** and **12** were examined for their ability to disrupt pre-formed, well-established staphylococcal biofilm using the microtiter plate biofilm formation assay[8]. The piperidine-containing derivatives **10** and **12** were both superior to vancomycin in their ability to disrupt the highly-resistant MRSA USA300 biofilm (Figure 6). Compound **10** exhibited the highest biofilm eradication activity as it eradicated about 72% of MRSA300 biofilm mass at 4 × MIC (16 µg/mL), while its 3-methyl analog **12** disrupted about 50% of MRSA USA300 biofilm mass, at the same concentration. On the other hand, vancomycin

at same concentration was unable to effectively penetrate and disrupt the mature biofilm because of its large molecular structure and polar nature, in agreement with previous reports [8, 49].

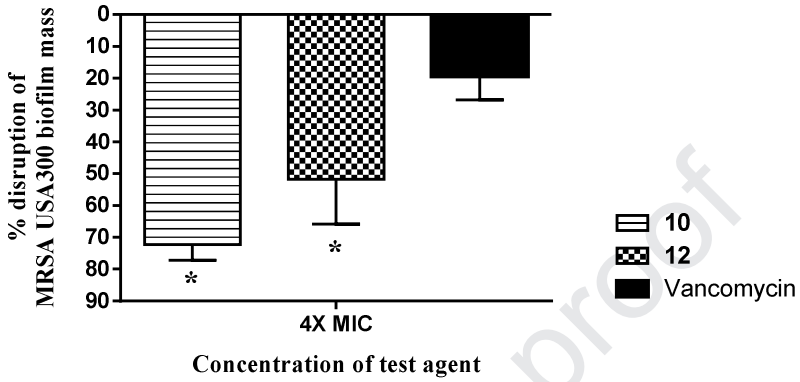

Figure 6. Disruption of mature MRSA biofilm by compounds 10, 12 and vancomycin at 4 × MIC. The data are presented as percent disruption of MRSA USA300 mature biofilm in relation to DMSO (the solvent for the compounds that served as a negative control). Vancomycin served as the control antibiotic. The values represent an average of four samples analyzed for each compound/antibiotic. Error bars represent standard deviation values. An asterisk (*) denotes statistical significance ($P < 0.05$) between results for test compounds relative to vancomycin analyzed via an unpaired Student's t-test.

3. Conclusion. Previously we have reported that cyclization of the *n*-butyl side chain of lead compound **1a** provided the more potent derivative **1b**. Though potency improved, compound **1b** was highly lipophilic and could not be tested in an *in vivo* model. The present study focused on increasing the drugability of the phenylthiazoles by controlling their physicochemical properties so that they can be formulated and tested in an animal model. This aim was achieved by using cyclic amines as the terminal side chain. Out of all tested derivatives, the piperidine and its 3-methyl analog (compounds **10** and **12**) provided the most promising candidates when tested against sixteen MDR clinical isolates. The new piperazine-containing phenylthiazoles **10** and **12** outperformed vancomycin in different aspects: being effective in disrupting MRSA biofilm mass, displaying efficient intracellular clearance activity against MRSA residing inside infected

macrophages, and exhibiting a fast-bactericidal activity against MRSA *in vitro*. More importantly, this series of antibacterial agents, represented by compound **10**, showed a significantly improved pharmacokinetic profile relative to the first-generation compounds. In this regard, compound **10** was orally absorbed and achieved a maximum plasma concentration more than two times higher than the compound's MIC values against MRSA. Additionally, unlike the metabolically unstable first-generation phenylthiazoles, compound **10** exhibited a high degree of metabolic stability with a half-life of 4 hours. The promising results obtained for compound **10** warrant further investigation in suitable animal models of MRSA infection, as part of a future study.

4. Experimental

4.1. Chemistry

4.1.1. General. ^{1}H NMR spectra were run at 400 MHz and ^{13}C spectra were determined at 100 MHz in deuterated dimethyl sulfoxide (DMSO-d_6) on a Varian Mercury VX-400 NMR spectrometer. Chemical shifts are given in parts per million (ppm) on the delta (δ) scale. Chemical shifts were calibrated relative to those of the solvents. Flash chromatography was performed on 230-400 mesh silica. The progress of reactions was monitored with Merck silica gel IB2-F plates (0.25 mm thickness). Mass spectra were recorded at 70 eV. High resolution mass spectra for all ionization techniques were obtained from a FinniganMAT XL95. Melting points were determined using capillary tubes with a Stuart SMP30 apparatus and are uncorrected. All yields reported refer to isolated yields. Compound (**3**) was prepared as reported.[22]

4.1.2. 1-(2-(4-(*Sec*-amine derivatives-1-yl)phenyl-4-methylthiazol-5-yl)ethan-1-one (4a-p).

General procedure: to dry DME (15 mL) and a few drops of distilled water in a 75-mL sealed tube compound **3** (300 mg, 1 mmol), palladium acetate (13 mg, 5 mol%), 2-

Journal Pre-proof

dicyclohexylphosphino-2',4',6'-triisopropylbiphenyl (**X**-phos) (56 mg, 10 mol%) and potassium *tert*-butoxide (336 mg, 2.5 equiv.). After the reaction mixture was purged with dry nitrogen gas for 15 min at 100 ^{o}C, appropriate *Sec*. amines (3 equiv.) were added. The sealed tube was then heated and stirred at 200 ^{o}C for 3 h and monitored by thin-layer chromatography (TLC). After completion of the reaction, the reaction mixture was poured on water then extracted with DCM (3 × 15 mL) then dried over $MgSO_4$, the organic materials were then concentrated under reduced pressure. The crude materials were purified via silica gel flash column chromatography using hexane-ethyl acetate (8:2) as yellowish viscous oil.

4.1.2.1. 1-(2-(4-(Azetidin-1-yl)phenyl)-4-methylthiazol-5-yl)ethan-1-one (4a). Orange oil (110 mg, 33.8%); ^{1}H NMR (DMSO-d_6) δ: 7.98 (d, *J* = 8.4 Hz, 2H), 7.57 (d, *J* = 8.4 Hz, 2H), 2.98 (t, *J* = 8 Hz, 4H), 2.69 (s, 3H), 2.43 (s, 3H), 1.98-1.97 (m, 2H); ^{13}C NMR (DMSO-d_6) δ: 191.05, 167.38, 161.69, 148.35, 143.23, 133.04, 132.98, 121.93, 52.53, 24.61, 18.08, 16.88; MS (*m*/*z*); 272 (M^+, 78.46%).

4.1.2.2. 1-(2-(4-(3-Hydroxyazitidin-1-yl)phenyl)-4-methylthiazol-5-yl)ethan-1-one (4b). Yellowish oil (95 mg, 27.6%); ^{1}H NMR (DMSO-d_6) δ: 7.89 (d, *J* = 8.4 Hz, 2H), 7.68 (d, *J* = 8.4 Hz, 2H), 4.56 (brs, 1H), 4.27-4.24 (m, 1H), 4.15 (dd, *J* = 12.1, 3.4, Hz, 2H), 3.62 (d, *J* = 12.2, 6.2 Hz, 2H), 2.59 (s, 3H), 2.47 (s, 3H); ^{13}C NMR (DMSO-d_6) δ: 192.95, 168.24, 163.66, 155.53, 149.84, 132.27, 127.19, 119.51, 64.44, 59.23, 31.36, 18.54; MS (*m/z*); 288 (M^+, 44.61%).

4.1.2.3. 1-(4-Methyl-2-(4-pyrrolidin-1-yl)phenyl)thiazol-5-yl)ethan-1-one (4c). Dark brown oil (120 mg, 35%); ^{1}H NMR (DMSO-d_6) δ: 7.88 (d, *J* = 8.8 Hz, 2H), 7.49 (d, *J* = 8.8 Hz, 2H), 3.52 (t, *J* = 6.8 Hz, 4H), 2.59 (s, 3H), 2.33 (s, 3H), 1.7 (t, *J* = 6.8 Hz, 4H); ^{13}C NMR (DMSO-d_6) δ: 191.45, 165.24, 160.14, 148.33, 143.93,133.14, 132.92, 121.91, 53.55, 29.47, 18.55, 16.61; MS (*m/z*); 286 (M^+, 54.20%).

4.1.2.4. 1-(4-Methyl-2-(4-(thiazolidin-3-yl)phenyl)thiazol-5-yl)ethan-1-one (4d). Yellow oil (96 mg, 26.4%); ^{1}H NMR (DMSO-d_6) δ: 7.97 (d, J = 8.1 Hz, 2H), 7.50 (d, J = 8.1 Hz, 2H), 4.51 (s, 2H), 3.74 (t, J = 6.4 Hz, 2H), 3.19 (t, J = 6.4 Hz, 2H), 2.62 (s, 3H), 2.48 (s, 3H); ^{13}C NMR (DMSO-d_6) δ: 191.66, 163.46, 158.83, 136.63, 132.44, 131.97, 126.14, 119.31, 60.26, 52.44, 29.86, 18.55, 16.76; MS (*m/z*); 304 (M^+, 45.03%).

4.1.2.5. 1-(2-(4-(1*H*-Imidazol-1-yl)phenyl)-4-methylthiazol-5-yl)ethan-1-one (4e). Brown oil (89 mg, 26.3%); ^{1}H NMR (DMSO-d_6) δ: 7.91 (d, J = 8.4 Hz, 2H), 7.68 (s, 1H), 7.57 (d, J = 8.4 Hz, 2H), 7.33 (d, J = 6.8 Hz, 1H), 6.98 (d, J = 6.8 Hz, 1H), 2.59 (s, 3H), 2.32 (s, 3H); ^{13}C NMR (DMSO-d_6) δ: 192.15, 164.34, 162.73, 136.93, 133.07, 132.94, 132.12, 131.91, 128.13, 124.63, 122.33, 29.86, 17.65; MS (*m/z*); 283 (M^+, 100%).

4.1.2.6. 1-(4-Methyl-2-(4-(piperidin-1-yl)phenyl)thiazol-5-yl)ethan-1-one (4f). Yellow oil (120 mg, 33.5%); ^{1}H NMR (DMSO-d_6) δ: 8.02 (d, J = 8.4 Hz, 2H), 7.51 (d, J = 8.4 Hz, 2H), 2.71 (s, 3H), 2.57 (s, 3H), 2.52 (t, J = 6.4 Hz, 4H), 1.57-1.51 (m, 4H), 1.39-1.36 (m, 2H); ^{13}C NMR (DMSO-d_6) δ: 191.35, 167.92, 158.56, 133.83, 132.54, 132.26, 127.25, 125.61, 53.10, 30.64, 25.94, 24.04, 18.45; MS (*m/z*); 300 (M^+, 40.55%).

4.1.2.7. 1-(4-Methyl-2-(4-(2-methylpiperidin-1-yl)phenyl)thiazol-5-yl)ethan-1-one (4g). Brown oil (95 mg, 25.3%); ^{1}H NMR (DMSO-d_6) δ: 7.98 (d, J = 8 Hz, 2H), 7.52 (d, J = 7.2 Hz, 2H), 3.83-3.81 (m, 1H), 3.16-2.86 (m, 2H), 2.54 (s, 3H), 2.38 (s, 3H), 1.60-1.22 (m, 6H), 1.05 (d, J = 6.8 Hz, 3H); ^{13}C NMR (DMSO-d_6) δ: 191.15, 168.12, 163.17, 158.83, 132.39, 132.54, 127.34, 126.08, 54.66, 53.39, 34.62, 30.69, 26.34, 24.76, 20.41, 18.31; MS (*m/z*); 314 (M^+, 15.74%).

4.1.2.8. 1-(4-Methyl-2-(4-(3-methylpiperidin-1-yl)phenyl)thiazol-5-yl)ethan-1-one (4h). Yellow oil (120 mg, 32%); ^{1}H NMR (DMSO-d_6) δ: 8.02 (d, J = 8.4 Hz, 2H), 7.57 (d, J = 8.4 Hz,

2H), 2.80-2.61 (m, 2H), 2.71 (s, 3H), 2.58 (s, 3H), 2.14-1.46 (m, 7H), 0.87 (d, *J* = 6.4 Hz, 3H); ^{13}C NMR (DMSO-d_6) δ: 191.34, 168.02, 158.89, 133.53, 133.22, 132.24, 127.11, 125.92, 60.35, 52.40, 48.01, 32.62, 30.99, 25.64, 18.94, 16.77; MS (*m/z*); 314 (M^+, 23.14%).

4.1.2.9. 1-(4-Methyl-2-(4-(4-methylpiperidin-1-yl)phenyl)thiazol-5-yl) ethan-1-one (4i). Light-yellow oil (150 mg, 40%); ^{1}H NMR (DMSO-d_6) δ: 7.88 (d, *J* = 8.4 Hz, 2H), 7.51 (d, *J* = 8.4 Hz, 2H), 2.84 (m, 4H), 2.59 (s, 3H), 2.31 (s, 3H), 2.20-2.12 (m, 4H), 1.61-1.11 (m, 1H), 0.90 (d, *J* = 6.4 Hz, 3H); ^{13}C NMR (DMSO-d_6) δ: 191.33, 168.84, 158.13, 147.33, 143.30, 132.44, 132.28, 122.31, 52.75, 34.71, 30.29, 26.24, 24.31, 16.84; MS (*m/z*); 314 (M^+, 21.14%).

4.1.2.10. 1-(4-Methyl-2-(4-(4-methylpiperazin-1-yl)phenyl)thiazol-5-yl)ethan-1-one (4j). Orange oil (160 mg, 42.5%); ^{1}H NMR (DMSO-d_6) δ: 8.01 (d, *J* = 8.4 Hz, 2H), 7.57 (d, *J* = 8.4 Hz, 2H), 3.62-3.54 (m, 4H), 2.72 (s, 3H), 2.59 (s, 3H), 2.52-2.49 (m, 4H), 2.16 (s, 3H); ^{13}C NMR (DMSO-d_6) δ: 191.18, 167.73, 158.63, 147.67, 143.62, 133.14, 132.43, 127.41, 55.15, 52.15, 46.01, 31.04, 18.74; MS (*m/z*); 315 (M^+, 24.14%).

4.1.2.11. 1-(2-(4-(4-Bromopiperidin-1-yl)phenyl)-4-methylthiazol-5-yl)ethan-1-one (4k). Yellow oil (200 mg, 44%); ^{1}H NMR (DMSO-d_6) δ: 7.49 (d, *J* = 8.4 Hz, 2H), 7.05 (d, *J* = 8.4 Hz, 2H), 4.43-4.12 (m, 1H), 3.62 (t, *J* = 6.4 Hz, 4H), 2.49 (s, 3H), 2.27 (s, 3H), 2.25-1.89 (m, 4H); ^{13}C NMR (DMSO-d_6) δ: 191.41, 161.54, 147.41, 144.43, 136.11, 132.04, 126.56, 124.12, 53.35, 34.41, 29.34, 18.34, 16.31; MS (*m/z*); 378 (M^+, 18.69%), 380 (M^{+2}, 19.36%).

4.1.2.12. 1-(4-Methyl-2-(4-morpholinophenyl)thiazol-5-yl)ethan-1-one (4l). Brown oil (150 mg, 41.6%); ^{1}H NMR (DMSO-d_6) δ: 7.79 (d, *J* = 8.4 Hz, 2H), 7.11 (d, *J* = 8.4 Hz, 2H), 3.62 (t, *J* = 6.4 Hz, 4H), 3.28 (t, *J* = 6.4 Hz, 4H), 2.64 (s, 3H), 2.36 (s, 3H); ^{13}C NMR (DMSO-d_6) δ: 191.53, 162.34, 154.91, 147.43, 132.88, 132.14, 126.16, 124.72, 64.15, 52.41, 28.15, 16.78; MS (*m/z*); 302 (M^+, 40.69%).

4.1.2.13. 1-(4-Methyl-2-(4-thiomorpholinophenyl)thiazol-5-yl)ethan-1-one (4m). Yellow oil (110 mg, 28.9%); ^{1}H NMR (DMSO-d_6) δ: 8.22 (d, *J* = 8.4 Hz, 2H), 7.81 (d, *J* = 8.4 Hz, 2H), 3.92 (t, *J* = 6.4 Hz, 4H), 3.75 (t, *J* = 6.4 Hz, 4H), 2.69 (s, 3H), 2.36 (s, 3H); ^{13}C NMR (DMSO-d_6) δ: 191.73, 166.34, 160.91, 157.73, 143.88, 133.14, 132.96, 122.62, 52.85, 28.85, 26.64, 16.78; MS (*m/z*); 318 (M^+, 42.69%).

4.1.2.14. 1-(2-(4-(Azepan-1-yl)phenyl)-4-methylthiazol-5-yl)ethan-1-one (4n). Dark-brown oil (100 mg, 26.6%); ^{1}H NMR (DMSO-d_6) δ: 8.26 (d, *J* = 8.4 Hz, 2H), 7.46 (d, *J* = 8.4 Hz, 2H), 4.43-4.38 (m, 4H), 2.52 (s, 3H), 2.46 (s, 3H), 1.55-0.96 (m, 8H); ^{13}C NMR (DMSO-d_6) δ: 190.95, 166.62, 160.86, 147.83, 143.74, 132.86, 132.25, 122.61, 53.19, 28.36, 26.64, 24.04, 18.35; MS (*m/z*); 314 (M^+, 27.60%).

4.1.2.15. 1-(2-(4-(Azocan-1-yl)phenyl)-4-methylthiazol-5-yl)ethan-1-one (4o). Brown oil (110 mg, 28%); ^{1}H NMR (DMSO-d_6) δ: 7.98 (d, *J* = 8.4 Hz, 2H), 7.16 (d, *J* = 8.4 Hz, 2H), 4.45 (t, *J* = 5.4 Hz, 4H), 2.62 (s, 3H), 2.46 (s, 3H), 1.89-0.86 (m, 10H); ^{13}C NMR (DMSO-d_6) δ: 191.35, 168.62, 163.86, 142.83, 133.74, 133.06, 126.65, 121.04, 53.26, 30.64, 30.02, 26.16, 24.84, 18.35; MS (*m/z*); 328 (M^+, 4.60%).

4.1.2.16. 1-(4-Methyl-2-(4-(octahydroisoquinolin-2(1*H*)-yl)phenyl)thiazol-5-yl)ethan-1-one (4p). Dark-brown oil (133 mg, 31.4%); ^{1}H NMR (DMSO-d_6) δ: 7.88 (d, *J* = 8.4 Hz, 2H), 7.51 (d, *J* = 8.4 Hz, 2H), 2.57-2.51 (m, 2H), 2.49-2.42 (m, 2H), 2.57 (s, 3H), 2.31 (s, 3H), 2.20-0.89 (m, 12H); ^{13}C NMR (DMSO-d_6) δ: 191.15, 160.42, 147.46, 133.33, 132.84, 128.76, 126.72, 124.62, 59.44, 53.58, 43.01, 42.68, 33.22, 30.34, 26.64, 18.41, 17.65; MS (*m/z*); 354 (M^+, 18.20%).

4.1.3. 2-(1-(2-(4-(Substituted *sec*-amine-1-yl)phenyl)-4-methylthiazol-5-yl)ethylidene)hydrazine-1-carboximidamide 5-20. ***General procedure***: Acetylphenylthiazole derivatives **4a-p** (0.31 mmol) were dissolved in absolute ethanol (15 mL), concentrated

hydrochloric acid (1 mL), aminoguanidine hydrochloride (175 mg, 1.5 mmol, 5 equiv.), were added. The reaction mixture was heated at reflux for 2 h. The solvent was concentrated under reduced pressure, then poured in crushed ice and neutralized with sodium carbonate to pH 7-8, and the formed precipitated was collected by filtration, washed with copious amount of water. Crystallization from absolute ethanol afforded the desired products as solids.

4.1.3.1. 2-(1-(2-(4-(Azetidin-1-yl)phenyl)-4-methylthiazol-5-yl)ethylidene)hydrazine-1-carbo- ximidamide (5). Yellow solid (90 mg, 75%); mp = 170-171 °C. ^{1}H NMR (DMSO -d_6) δ: 11.49 (brs, 1H), 7.77 (d, *J* = 8.4 Hz, 2H), 7.21 (d, *J* = 8.4 Hz, 2H), 4.11 (brs, 3H), 3.52 (t, *J* = 5.2 Hz, 4H), 2.62 (s, 3H), 2.49 (s, 3H), 2.13-2.02 (m, 2H); ^{13}C NMR (DMSO-d_6) δ: 169.08, 165.42, 158.83, 147.51, 133.06, 132.61, 132.18, 126.94, 125.97, 49.76, 31.11, 18.44, 16.37; HRMS (EI) *m/z* 328.1478 M^+, calc. for $C_{16}H_{20}N_6S$ 328.1470 M^+; Anal. Calc. for: $C_{16}H_{20}N_6S$ (328): C, 58.51; H, 6.14; N, 25.59%; Found: C, 58.53; H, 6.09; N, 25.60%.

4.1.3.2. 2-(1-(2-(4-(3-Hydroxyazetidin-1-yl)phenyl)-4-methylthiazol-5-yl)ethylidene) hydrazine-1-carboximidamide (6). Orange solid (105 mg, 88%); mp = 191-192 °C. ^{1}H NMR (DMSO -d_6) δ: 7.65 (d, *J* = 8.4 Hz, 2H), 7.05 (brs, 1H), 6.68 (d, *J* = 8.4 Hz, 2H), 6.21 (brs, 3H), 5.48 (brs, 1H), 3.81-3.78 (m, 1H), 3.75 (dd, *J* = 11.3, 3.4 Hz, 2H), 3.70 (dd, *J* = 11.4, 6.2 Hz, 2H), 2.51 (s, 3H), 2.36 (s, 3H); ^{13}C NMR (DMSO-d_6) δ: 168.77, 162.42, 158.83, 155.42, 148.89, 133.17, 132.78, 127.13, 126.77, 63.35, 58.43, 31.11, 18.49; HRMS (EI) *m/z* 344.1399 M^+, calc. for $C_{16}H_{20}N_6OS$ 344.1419 M^+; Anal. Calc. for: $C_{16}H_{20}N_6OS$ (344): C, 55.79; H, 5.85; N, 24.40%; Found: C, 55.81; H, 5.91; N, 24.48%.

4.1.3.3. 2-(1-(4-Methyl-2-(4-(pyrrolidin-1-yl)phenyl)thiazol-5-yl)ethylidene)hydrazine-1-carboximidamide (7). Brown solid (174 mg, 74%); mp = 166-168 °C. ^{1}H NMR (DMSO -d_6) δ: 7.77 (d, *J* = 7.2 Hz, 2H), 7.50 (d, *J* = 7.2 Hz, 2H), 5.52 (brs, 2H), 5.48 (brs, 2H), 3.64-3.57 (m,

4H), 2.57 (s, 3H), 2.31 (s, 3H), 1.71-1.62 (m, 4H); ^{13}C NMR (DMSO-d_6) δ: 162.57, 161.14, 148.74, 143.19, 136.08, 133.16, 132.67, 126.22, 124.18, 52.49, 23.67, 18.73, 16.55; HRMS (EI) *m/z* 342.1641 M^+, calc. for $C_{17}H_{22}N_6S$ 342.1627M^+; Anal. Calc. for: $C_{17}H_{22}N_6S$ (342): C, 59.62; H, 6.48; N, 24.54%; Found: C, 59.66; H, 6.52; N, 24.61%.

4.1.3.4. 2-(1-(4-Methyl-2-(4-(thiazolidin-3-yl)phenyl)thiazol-5-yl)ethylidene)hydrazine-1-carboximidamide (8). Yellow solid (67 mg, 65.7%); mp = 177-179 °C. ^{1}H NMR (DMSO -d_6) δ: 8.05 (d, *J* = 8.4 Hz, 2H), 7.81 (brs, 4H), 7.72 (d, *J* = 8.4 Hz, 2H), 4.65 (s, 2H), 3.23 (t, *J* = 6.4 Hz, 2H), 2.81 (t, *J* = 6.4 Hz, 2H), 2.62 (s, 3H), 2.45 (s, 3H); ^{13}C NMR (DMSO-d_6) δ: 168.54, 164.94, 158.74, 147.79, 137.18, 132.16, 131.87, 127.12, 125.64, 62.33, 55.45, 31.27, 22.43, 18.65; HRMS (EI) *m/z* 360.1185 M^+, calc. for $C_{16}H_{20}N_6S_2$ 360.1191 M^+; Anal. Calc. for: $C_{16}H_{20}N_6S_2$ (360): C, 53.31; H, 5.59; N, 23.31%; Found: C, 53.35; H, 5.63; N, 23.36%.

4.1.3.5. 2-(1-(2-(4-(1*H*-Imidazol-1-yl)phenyl)-4-methylthiazol-5-yl)ethylidene)hydrazine-1-carboximidamide (9). Brown solid (71 mg, 59%); mp = 183-185 °C. ^{1}H NMR (DMSO -d_6) δ: 7.89 (d, *J* = 8.4 Hz, 2H), 7.68 (s, 1H), 7.54 (d, *J* = 8.4 Hz, 2H), 7.33 (d, *J* = 7.2 Hz, 1H), 6.93 (d, *J* = 7.2 Hz, 1H), 5.66 (brs, 2H), 5.54 (brs, 2H), 5.22 (s, 2H), 2.58 (s, 3H), 2.32 (s, 3H); ^{13}C NMR (DMSO-d_6) δ: 165.25, 158.63, 154.63, 134.93, 134.74, 133.52, 132.91, 128.53, 127.43, 126.85, 122.46, 124.33, 30.50, 18.55; HRMS (EI) *m/z* 339.1250 M^+, calc. for $C_{16}H_{17}N_7S$ 339.1266 M^+; Anal. Calc. for: $C_{16}H_{17}N_7S$ (339): C, 56.62; H, 5.05; N, 28.89%; Found: C, 56.70; H, 5.09; N, 28.94%.

4.1.3.6. 2-(1-(4-Methyl-2-(4-(piperidin-1-yl)phenyl)thiazol-5-yl)ethylidene)hydrazine-1-carboximidamide (10). Yellow solid (86 mg, 72.8%); mp = 192-194 °C. ^{1}H NMR (DMSO -d_6) δ: 11.51 (brs, 1H), 8.01 (d, *J* = 8.4 Hz, 2H), 7.82 (brs, 3H), 7.64 (d, *J* = 8.4 Hz, 2H), 3.55-3.49 (m, 4H), 3.02-3.95 (m, 4H), 2.62 (s, 3H), 2.42 (s, 3H), 1.84-1.76 (m, 2H); ^{13}C NMR (DMSO-d_6)

Journal Pre-proof

δ: 167.84, 160.23, 156.42, 147.39, 133.10, 132.27, 127.53, 125.94, 119.87, 53.47, 31.91, 26.23, 24.91, 18.75; HRMS (EI) *m/z* 356.1795 M^+, calc. for $C_{18}H_{24}N_6S$ 356.1783 M^+; Anal. Calc. for: $C_{18}H_{24}N_6S$ (356): C, 60.65; H, 6.79; N, 23.57%; Found: C, 60.69; H, 6.85; N, 23.62%.

4.1.3.7. 2-(1-(4-Methyl-2-(4-(2-methylpiperidin-1-yl)phenyl)thiazol-5-yl)ethylidene) hydrazine-1-carboximidamide (11). Yellow solid (65 mg, 55.5%); mp = 189-191 °C. ^{1}H NMR (DMSO -d_6) δ: 7.89 (d, *J* = 8.4 Hz, 2H), 7.51 (d, *J* = 8.4 Hz, 2H), 5.78 (brs, 4H), 3.74-3.58 (m, 2H), 3.52-3.49 (m, 1H), 2.59 (s, 3H), 2.33 (s, 3H), 1.61-1.19 (m, 6H), 1.06 (d, *J* = 4.8 Hz, 3H); ^{13}C NMR (DMSO-d_6) δ: 162.59, 161.15, 148.75, 143.44, 137.43, 133.19, 132.78, 126.33, 124.91, 54.82, 53.26, 34.63, 26.22, 24.96, 20.13, 18.79, 16.69; HRMS (EI) *m/z* 370.1944 M^+, calc. for $C_{19}H_{26}N_6S$ 370.1940 M^+; Anal. Calc. for: $C_{19}H_{26}N_6S$ (370): C, 61.59; H, 7.07; N, 22.68%; Found: C, 61.62; H, 7.11; N, 22.74%.

4.1.3.8. 2-(1-(4-Methyl-2-(4-(3-(methylpiperidin-1-yl)phenyl)thiazol-5-yl)ethylidene) hydrazine-1-carboximidamide (12). Yellow-white solid (80 mg, 68%); mp = 195-196 °C. ^{1}H NMR (DMSO -d_6) δ: 7.79 (d, *J* = 8.4 Hz, 2H), 7.42 (d, *J* = 8.4 Hz, 2H), 5.77 (brs, 2H), 5.47 (brs, 2H), 3.27 (d, *J* = 9.6 Hz, 2H), 3.19-3.09 (m, 2H), 2.61 (s, 3H), 2.46 (s, 3H), 2.12-1.36 (m, 5H), 1.56 (d, *J* = 6.4 Hz, 3H); ^{13}C NMR (DMSO-d_6) δ: 168.51, 163.25, 158.75, 147.33, 132.78, 132.11, 127.53, 125.87, 122.61, 54.72, 53.26, 34.73, 31.22, 25.71, 24.56, 18.53, 16.89; HRMS (EI) *m/z* 370.1930 M^+, calc. for $C_{19}H_{26}N_6S$ 370.1940 M^+; Anal. Calc. for: $C_{19}H_{26}N_6S$ (370): C, 61.59; H, 7.07; N, 22.68%; Found: C, 61.62; H, 7.11; N, 22.74%.

4.1.3.9. 2-(1-(4-Methyl-2-(4-(4-(methylpiperidin-1-yl)phenyl)thiazol-5-yl)ethylidene) hydrazine-1-carboximidamide (13). Yellow solid (90 mg, 76.9%); mp = 201-202 °C. ^{1}H NMR (DMSO -d_6) δ: 11.41 (brs, 1H), 7.78 (d, *J* = 8 Hz, 2H), 7.51 (brs, 3H), 7.27 (d, *J* = 8 Hz, 2H), 2.61 (s, 3H), 2.31 (s, 3H), 2.18 (t, *J* = 12 Hz, 4H), 1.62 (t, *J* = 10.8 Hz, 4H), 1.32-1.27 (m, 1H),

0.89 (d, *J* = 6.4 Hz, 3H); ^{13}C NMR (DMSO-d_6) δ: 161.61, 160.19, 148.72, 143.41, 136.18, 132.90, 132.02, 126.10, 124.47, 52.52, 34.65, 30.16, 22.34, 18.75, 16.39; HRMS (EI) *m/z* 370.1940 M^+, calc. for $C_{19}H_{26}N_6S$ 370.1933 M^+; Anal. Calc. for: $C_{19}H_{26}N_6S$ (370): C, 61.59; H, 7.07; N, 22.68%; Found: C, 61.62; H, 7.11; N, 22.74%.

4.1.3.10. 2-(1-(4-Methyl-2-(4-(4-(4-methylpiperazin-1-yl)phenyl)thiazol-5-yl)ethylidene) hydrazine-1-carboximidamide (14). Orange solid (77 mg, 65%); mp = 175-176 °C. ^{1}H NMR (DMSO -d_6) δ: 7.99 (d, *J* = 8.8 Hz, 2H), 7.57 (d, *J* = 8.8 Hz, 2H), 5.75 (brs, 4H), 4.75-4.69 (m, 4H), 2.52 (s, 3H), 2.45 (s, 3H), 2.31-2.25 (m, 4H), 2.21 (s, 3H); ^{13}C NMR (DMSO-d_6) δ: 168.28, 165.09, 158.65, 146.11, 143.58, 133.45, 132.88, 127.21, 125.93, 56.01, 46.03, 45.13, 30.28, 18.55; HRMS (EI) *m/z* 371.1901 M^+, calc. for $C_{18}H_{25}N_7S$ 371.1892 M^+; Anal. Calc. for: $C_{18}H_{25}N_7S$ (371): C, 58.19; H, 6.78; N, 26.39%; Found: C, 58.25; H, 6.84; N, 26.45%.

4.1.3.11. 2-(1-(2-(4-(4-Bromopiperidin-1-yl)phenyl)-4-methylthiazol-5-yl)ethylidene) hydrazine-1-carboximidamide (15). Yellow solid (96 mg, 84%); ^{1}H NMR (DMSO-d_6) δ: 7.49 (d, *J* = 8.4 Hz, 2H), 7.02 (d, *J* = 8.4 Hz, 2H), 5.21 (brs, 2H), 5.07 (brs, 2H), 4.62-4.54 (m, 1H), 3.42 (t, *J* = 6.4 Hz, 4H), 2.49 (s, 3H), 2.27 (s, 3H), 2.25-1.89 (m, 4H); ^{13}C NMR (DMSO-d_6) δ: 162.54, 160.96, 148.41, 144.53, 136.21, 132.04, 131.83, 126.56, 124.12, 53.55, 48.11, 34.51, 29.44, 18.34, 16.21; HRMS (EI) *m/z* 434.0890 M^+, calc. for $C_{18}H_{23}BrN_6S$ 434.0888 M^+, 436.0868 M^+ Anal. Calc. for: $C_{18}H_{23}$ BrN_7S (435): C, 49.66; H, 5.32; N, 19.30%; Found: C, 49.70; H, 5.35; N, 19.37%.

4.1.3.12. 2-(1-(4-Methyl-2-(4-morpholinophenyl)thiazol-5-yl)ethylidene)hydrazine-1-carboximid-amide (16). Brown solid (87 mg, 73%); mp = 186-187 °C. ^{1}H NMR (DMSO -d_6) δ: 8.01 (d, *J* = 8.4 Hz, 2H), 7.65 (d, *J* = 8.4 Hz, 2H), 5.65 (brs, 2H), 5.48 (brs, 2H), 3.87-3.81 (m, 4H), 3.65-3.60 (m, 4H), 2.71 (s, 3H), 2.57 (s, 3H); ^{13}C NMR (DMSO-d_6) δ: 167.28, 162.49,

154.75, 147.37, 142.18, 133.98, 132.45, 126.21, 124.95, 64.11, 52.23, 27.18, 16.55; HRMS (EI) *m/z* 358.1595 M^+, calc. for $C_{17}H_{22}N_6OS$ 358.1576 M^+; Anal. Calc. for: $C_{17}H_{22}N_6OS$ (358): C, 56.96; H, 6.19; N, 23.45%; Found: C, 57.01; H, 6.25; N, 23.55%.

4.1.3.13. 2-(1-(4-Methyl-2-(4-thiomorpholinophenyl)thiazol-5-yl)ethylidene)hydrazine-1-carboximid-amide (17). Yellow solid (68 mg, 58%); mp = 194-196 °C. ^{1}H NMR (DMSO -d_6) δ: 8.25 (d, *J* = 8.4 Hz, 2H), 7.75 (d, *J* = 8.4 Hz, 2H), 5.60 (brs, 4H), 3.98-3.91 (m, 4H), 3.81-3.77 (m, 4H), 2.69 (s, 3H), 2.41 (s, 3H); ^{13}C NMR (DMSO-d_6) δ: 162.11, 160.09, 147.75, 143.37, 136.78, 132.45, 132.05, 126.41, 124.85, 56.23, 30.23, 18.38, 16.65; HRMS (EI) *m/z* 374.1349 M^+, calc. for $C_{17}H_{22}N_6S_2$ 374.1347 M^+; Anal. Calc. for: $C_{17}H_{22}N_6S_2$ (374): C, 54.52; H, 5.92; N, 22.44%; Found: C, 54.61; H, 5.99; N, 22.51%.

4.1.3.14. 2-(1-(2-(4-(Azepan-1-yl)phenyl)-4-methylthiazol-5-yl)ethylidene)hydrazine-1-carboximid-amide (18). Brown solid (65 mg, 55.5%); mp = 166-168 °C. ^{1}H NMR (DMSO -d_6) δ: 7.98 (d, *J* = 8.4 Hz, 2H), 7.49 (d, *J* = 8.4 Hz, 2H), 5.53 (brs, 2H), 5.45 (brs, 2H), 4.35 (t, *J* = 6.8 Hz, 4H), 2.71 (s, 3H), 2.44 (s, 3H), 1.95-1.05 (m, 8H); ^{13}C NMR (DMSO-d_6) δ: 167.49, 164.45, 158.36, 149.75, 136.93, 132.79, 132.18, 127.23, 125.11, 53.26, 31.71, 26.33, 24.70, 18.69; HRMS (EI) *m/z* 370.1923 M^+, calc. for $C_{19}H_{26}N_6S$ 370.1940 M^+; Anal. Calc. for: $C_{19}H_{26}N_6S$ (370): C, 61.59; H, 7.07; N, 22.68%; Found: C, 61.67; H, 7.11; N, 22.74%.

4.1.3.15. 2-(1-(2-(4-(Azocan-1-yl)phenyl)-4-methylthiazol-5-yl)ethylidene)hydrazine-1-carboximid-amide (19). Brown solid (60 mg, 51%); mp = 167-169 °C. ^{1}H NMR (DMSO -d_6) δ: 7.78 (d, *J* = 8.4 Hz, 2H), 7.53 (d, *J* = 8.4 Hz, 2H), 5.76 (brs, 2H), 5.56 (brs, 2H), 4.44 (t, *J* = 6.8 Hz, 4H), 2.75 (s, 3H), 2.44 (s, 3H), 1.95-1.09 (m, 8H), 0.88 (d, *J* = 6.4 Hz, 2H); ^{13}C NMR (DMSO-d_6) δ: 163.49, 161.75, 148.86, 143.45, 136.43, 133.29, 129.48, 126.23, 124.41, 47.11, 34.21, 30.13, 26.10, 25.76, 18.49, 16.66; HRMS (EI) *m/z* 384.2094 M^+, calc. for $C_{20}H_{28}N_6S$

Journal Pre-proof

384.2096 M^+; Anal. Calc. for: $C_{20}H_{28}N_6S$ (384): C, 62.47; H, 7.34; N, 21.85%; Found: C, 62.55; H, 7.38; N, 21.93%.

4.1.3.16. 2-(1-(4-Methyl-2-(4-(octahydroisoquinolin-2(1*H*)-yl)phenyl)thiazol-5-yl)ethylidene) hydrazine-1-carboximidamide (20). Yellow solid (69 mg, 59%); mp = 177-179 °C. ^{1}H NMR (DMSO -d_6) δ: 7.85 (d, *J* = 8.4 Hz, 2H), 7.51 (d, *J* = 8.4 Hz, 2H), 5.76 (brs, 2H), 5.68 (brs, 2H), 2.72 (t, *J* = 10.8 Hz, 2H), 2.68 (d, *J* = 8.8 Hz, 2H), 2.59 (s, 3H), 2.31 (s, 3H), 2.22-0.92 (m, 12H); ^{13}C NMR (DMSO-d_6) δ: 162.11, 160.06, 148.96, 143.77, 136.48, 132.53, 129.39, 126.49, 124.17, 59.32, 56.89, 47.69, 43.95, 34.25, 30.60, 26.60, 26.17, 18.65, 16.57; HRMS (EI) *m/z* 410.2265 M^+, calc. for $C_{22}H_{30}N_6S$ 410.2253 M^+; Anal. Calc. for: $C_{22}H_{30}N_6S$ (410): C, 64.36; H, 7.37; N, 20.47%; Found: C, 64.40; H, 7.41; N, 20.52%.

4.2. Microbiological assays

4.2.1. Bacterial strains, mammalian cell lines and antibiotics. Bacterial strains used in this study were obtained from Biodefense and Emerging Infections Research Resources Repository (BEI Resources) and the American Type Culture Collection (ATCC). Human colorectal adenocarcinoma (Caco-2) cell line, human keratinocyte cell line (HaCaT) and murine macrophage (J774) cells were purchased from American Type Culture Collection (ATCC). Linezolid (Chem-impex International, Wood Dale, IL, USA) and vancomycin hydrochloride (Gold Biotechnology, St. Louis, MO, USA), were purchased from commercial vendors. Phenylthiazole compounds were prepared in a stock concentration of 10 mg/mL in DMSO.

4.2.2. Determination of MICs and MBCs of the new phenylthiazole compounds against *Staphylococcus aureus* and other multidrug-resistant Gram-positive bacterial species. The broth microdilution method was utilized to test the antibacterial activity of the new phenylthiazole compounds against a panel of clinically-important *S. aureus* strains and Gram-

Journal Pre-proof

positive bacteria. The minimum inhibitory concentration (MIC) of teste compounds and control antibiotics (linezolid, and vancomycin) was determined using the broth microdilution method against methicillin-sensitive *Staphylococcus aureus* (ATCC 6538 and NRS107), methicillin-resistant *Staphylococcus aureus* (MRSA) and vancomycin-resistant *Staphylococcus aureus* (VRSA) clinical isolates according to the guidelines outlined by the Clinical and Laboratory Standards Institute (CLSI) [50]. Bacterial strains were grown aerobically overnight on tryptone soy agar plates at 37° C. Afterwards, a bacterial solution equivalent to 0.5 McFarland standard was prepared and diluted in cation-adjusted Mueller-Hinton broth (CAMHB) to achieve a bacterial concentration of about 5×10^5 CFU/mL and seeded in 96-well plates. Compounds and control drugs were added in the first row of the 96-well plates and serially diluted along the plates. Plates were then, incubated aerobically at 37° C for 18-20 hours. MICs reported in here are the minimum concentration of the compounds and control drugs that could completely inhibit the visual growth of bacteria. The minimum bactericidal concentration (MBC) of these compounds was tested by plating 4 µL from wells with no growth onto Tryptic soy agar plates. Plates were incubated at 37 ºC for 18-20 hours before recording the MBC. The MBC was categorized as the lowest concentration that reduced bacterial growth by 99.9%.

4.2.3. In vitro cytotoxicity analysis of compounds 10 and 12 against human colorectal, human keratinocyte and murine macrophage cells. Phenylthiazoles **10** and **12** were assayed for potential cytotoxicity against a human colorectal adenocarcinoma (Caco-2) cell line, human keratinocyte cell line (HaCaT) and murine macrophage (J774) cells, as described previously [5]. Briefly, tested compounds were incubated with caco-2 and HaCaT cells for 2 hours, and with J774 cells for 24 hours. Then, cells were incubated with MTS 3-(4,5-dimethylthiazol-2-yl)-5-(3-

carboxymethoxyphenyl)-2-(4-sulfophenyl)-2H-tetrazolium) reagent for 4 hours before measuring absorbance values (OD_{490}).

4.2.4. MRSA biofilm eradication assessment. Phenylthiazole compounds **10** and **12** were examined for their ability to eradicate pre-formed, well established mature staphylococcal biofilm using the microtiter plate biofilm formation assay as described in previous reports [8, 51]. An overnight culture of MRSA USA300 (NRS384) was diluted 1:100 in culture medium (Tryptic soy broth + 1% glucose). For detection of biofilm eradication, bacterial suspension was added, and plates were incubated at 37 °C for 24 hours in order to form a strong adherent biofilm. The bacterial suspension (planktonic cells) was removed and compounds were added at concentrations ranging from 256 to 2 µg/mL in Tryptic soy broth. Plates were incubated at 37 °C for 24 hours. In order to quantify biofilm mass, the bacterial suspension was removed, and wells were washed with phosphate-buffered saline to remove planktonic bacteria. An aliquot of 0.1% crystal violet was added to each well to stain the attached biofilm mass. After 30 minutes, wells were washed with sterile water and dried. Wells were de-stained using 100% ethanol prior to quantifying biofilm mass using a spectrophotometer (OD_{595}). Data are presented as percent eradication of MRSA USA300 biofilm for each test agent relative to the negative (DMSO) control wells. Data were analyzed using unpaired t test ($P < 0.05$).

4.2.5. Intracellular infection of J774 cells with MRSA and treatment with compound 10. The ability of compound **10** and vancomycin (at 2 × MIC) to reduce the burden of intracellular MRSA USA400 inside murine macrophage (J774) cells was evaluated. In brief, murine macrophage cells (J774) were cultured in Dulbecco's Modified Eagle Medium (DMEM) supplemented with 10% FBS at 37°C with CO_2 (5%). J774 cells were exposed to MRSA USA400 cells at a multiplicity of infection of approximately 10:1. After 1 hour of infection, J774

Journal Pre-proof

cells were washed with gentamicin (100 µg/mL) to kill extracellular MRSA. The compounds or vancomycin (at 2x MIC) were subsequently added to each well (four replicates per test agent). Control cells received DMSO at a concentration equal to that in drug-treated cell samples. After 24 hours incubation at 37°C with 5% CO_2, the test agents were removed. J774 cells were washed and subsequently lysed using 0.1% Triton-X. The solution was serially diluted in phosphate-buffered saline and transferred to TSA plates in order to determine viable MRSA CFU inside the J774 cells. Plates were incubated at 37ºC for 18-22 hour before counting viable CFU/mL. Statistical significance was assessed with one-way ANOVA, with post hoc Dunnet's multiple comparisons test ($P < 0.05$), utilizing GraphPad Prism 6.0 (GraphPad Software, La Jolla, CA).

4.2.6. Killing kinetics of compounds 10 and 12 against MRSA. The test was performed against MRSA USA400, as described previously.[2] Briefly, logarithmic phase bacterial cells were diluted, and drugs were added at 5 × MIC (in triplicates). At the corresponding time intervals, bacterial cells were diluted and plated on Tryptic soy agar plates to determine the viable colony forming unit (CFU)/mL.

4.3. *In vivo* Pharmacokinetics. Pharmacokinetic studies were performed in male naïve Sprague −Dawley (SD) rats, (three animals) following Institutional Animal Care and Use Committee guidelines. Oral dosing (50 mg/kg) was administered by gavage in a vehicle containing 2% ethanol, 48% PEG 400, and 50% water. Blood samples were collected over a 12-hour period post dose into Vacutainer tubes containing EDTA-K2. Plasma was isolated, and the concentration of compound **10** in plasma was determined with LC/MS/MS after protein precipitation with acetonitrile. Non-compartmental pharmacokinetic analysis was performed on plasma concentration data to calculate pharmacokinetic parameters a previous report [13].

Journal Pre-proof

Journal Pre-proof

Acknowledgement. This work was funded by Science & Technology Development Funds (STDF-Egypt) and the Egyptian Ministry of Higher Education and Scientific Research (MHESR). Article is derived from the Subject Data funded in whole or part by NAS and USAID, and that any opinions, findings, conclusions, or recommendations expressed in such article are those of the authors alone, and do not necessarily reflect the views of USAID or NAS.

References

[1] I. Eid, M.M. Elsebaei, H. Mohammad, M. Hagras, C.E. Peters, Y.A. Hegazy, B. Cooper, J. Pogliano, K. Pogliano, H.S. Abulkhair, M.N. Seleem, A.S. Mayhoub, Arylthiazole antibiotics targeting intracellular methicillin-resistant Staphylococcus aureus (MRSA) that interfere with bacterial cell wall synthesis, Eur J Med Chem, 139 (2017) 665-673.

[2] M. ElAwamy, H. Mohammad, A. Hussien, N.S. Abutaleb, M. Hagras, R.A.T. Serya, A.T. Taher, K.A. Abouzid, M.N. Seleem, A.S. Mayhoub, Alkoxyphenylthiazoles with broad-spectrum activity against multidrug-resistant gram-positive bacterial pathogens, Eur J Med Chem, 152 (2018) 318-328.

[3] M. Hagras, N.S. Abutaleb, A.O. Ali, J.A. Abdel-Aleem, M.M. Elsebaei, M.N. Seleem, A.S. Mayhoub, Naphthylthiazoles: Targeting Multidrug-Resistant and Intracellular Staphylococcus aureus with Biofilm Disruption Activity, ACS Infect Dis, 4 (2018) 1679-1691.

[4] M.M. Elsebaei, H. Mohammad, A. Samir, N.S. Abutaleb, A.B. Norvil, A.R. Michie, M.M. Moustafa, H. Samy, H. Gowher, M.N. Seleem, A.S. Mayhoub, Lipophilic efficient phenylthiazoles with potent undecaprenyl pyrophosphatase inhibitory activity, Eur J Med Chem, 175 (2019) 49-62.

Journal Pre-proof

[5] A. Kotb, N.S. Abutaleb, M.A. Seleem, M. Hagras, H. Mohammad, A. Bayoumi, A. Ghiaty, M.N. Seleem, A.S. Mayhoub, Phenylthiazoles with tert-Butyl side chain: Metabolically stable with anti-biofilm activity, Eur J Med Chem, 151 (2018) 110-120.

[6] M. Hagras, Y.A. Hegazy, A.H. Elkabbany, H. Mohammad, A. Ghiaty, T.M. Abdelghany, M.N. Seleem, A.S. Mayhoub, Biphenylthiazole antibiotics with an oxadiazole linker: An approach to improve physicochemical properties and oral bioavailability, Eur J Med Chem, 143 (2018) 1448-1456.

[7] M. Hagras, H. Mohammad, M.S. Mandour, Y.A. Hegazy, A. Ghiaty, M.N. Seleem, A.S. Mayhoub, Investigating the Antibacterial Activity of Biphenylthiazoles against Methicillin- and Vancomycin-Resistant Staphylococcus aureus (MRSA and VRSA), J Med Chem, 60 (2017) 4074-4085.

[8] H. Mohammad, A.S. Mayhoub, M. Cushman, M.N. Seleem, Anti-biofilm activity and synergism of novel thiazole compounds with glycopeptide antibiotics against multidrug-resistant staphylococci, J Antibiot (Tokyo), 68 (2015) 259-266.

[9] H. Mohammad, A.S. Mayhoub, A. Ghafoor, M. Soofi, R.A. Alajlouni, M. Cushman, M.N. Seleem, Discovery and characterization of potent thiazoles versus methicillin- and vancomycin-resistant Staphylococcus aureus, J Med Chem, 57 (2014) 1609-1615.

[10] H. Mohammad, P.V. Reddy, D. Monteleone, A.S. Mayhoub, M. Cushman, G.K. Hammac, M.N. Seleem, Antibacterial Characterization of Novel Synthetic Thiazole Compounds against Methicillin-Resistant Staphylococcus pseudintermedius, PLoS One, 10 (2015) e0130385.

[11] H. Mohammad, P.V. Reddy, D. Monteleone, A.S. Mayhoub, M. Cushman, M.N. Seleem, Synthesis and antibacterial evaluation of a novel series of synthetic phenylthiazole compounds

Journal Pre-proof

against methicillin-resistant Staphylococcus aureus (MRSA), Eur J Med Chem, 94 (2015) 306-316.

[12] H. Mohammad, W. Younis, H.G. Ezzat, C.E. Peters, A. AbdelKhalek, B. Cooper, K. Pogliano, J. Pogliano, A.S. Mayhoub, M.N. Seleem, Bacteriological profiling of diphenylureas as a novel class of antibiotics against methicillin-resistant Staphylococcus aureus, PLoS One, 12 (2017) e0182821.

[13] M.A. Seleem, A.M. Disouky, H. Mohammad, T.M. Abdelghany, A.S. Mancy, S.A. Bayoumi, A. Elshafeey, A. El-Morsy, M.N. Seleem, A.S. Mayhoub, Second-Generation Phenylthiazole Antibiotics with Enhanced Pharmacokinetic Properties, J Med Chem, 59 (2016) 4900-4912.

[14] E. Yahia, H. Mohammad, T.M. Abdelghany, E. Fayed, M.N. Seleem, A.S. Mayhoub, Phenylthiazole antibiotics: A metabolism-guided approach to overcome short duration of action, Eur J Med Chem, 126 (2017) 604-613.

[15] A. AbdelKhalek, N.S. Abutaleb, H. Mohammad, M.N. Seleem, Repurposing ebselen for decolonization of vancomycin-resistant enterococci (VRE), Plos One, 13 (2018) e0199710.

[16] H. Mohammad, W. Younis, L. Chen, C.E. Peters, J. Pogliano, K. Pogliano, B. Cooper, J. Zhang, A. Mayhoub, E. Oldfield, M. Cushman, M.N. Seleem, Phenylthiazole Antibacterial Agents Targeting Cell Wall Synthesis Exhibit Potent Activity in Vitro and in Vivo against Vancomycin-Resistant Enterococci, J Med Chem, 60 (2017) 2425-2438.

[17] H. Patil, R.V. Tiwari, M.A. Repka, Hot-melt extrusion: from theory to application in pharmaceutical formulation, AAPS PharmSciTech, 17 (2016) 20-42.

[18] R.V. Tiwari, H. Patil, M.A. Repka, Contribution of hot-melt extrusion technology to advance drug delivery in the 21st century, Expert Opin Drug Deliv, 13 (2016) 451-464.

[19] E. Mogalian, R. Oliyai, D. Stefanidis, V. Zia, Solid dispersion formulation of an antiviral compound, in, Google Patents, 2014.

[20] M.M. Hann, Molecular obesity, potency and other addictions in drug discovery, MedChemComm, 2 (2011) 349-355.

[21] P.D. Leeson, B. Springthorpe, The influence of drug-like concepts on decision-making in medicinal chemistry, Nat Rev Drug Discov, 6 (2007) 881.

[22] A.S. Mayhoub, M. Khaliq, R.J. Kuhn, M. Cushman, Design, synthesis, and biological evaluation of thiazoles targeting flavivirus envelope proteins, J Med Chem, 54 (2011) 1704-1714.

[23] S. Sonoda, T. Yamaguchi, K. Aoki, D. Ono, A. Sato, C. Kajiwara, S. Kimura, Y. Akasaka, Y. Ishii, Y. Miyazaki, N. Inase, K. Tateda, Evidence of latent molecular diversity determining the virulence of community-associated MRSA USA300 clones in mice, Immun Inflamm Dis, 6 (2018) 402-412.

[24] I.A. Tickler, R.V. Goering, J.R. Mediavilla, B.N. Kreiswirth, F.C. Tenover, H.A.I. Consortium, Continued expansion of USA300-like methicillin-resistant Staphylococcus aureus (MRSA) among hospitalized patients in the United States, Diagn Microbiol Infect Dis, 88 (2017) 342-347.

[25] C.B. Long, R.P. Madan, B.C. Herold, Diagnosis and management of community-associated MRSA infections in children, Expert Rev Anti-Infe, 8 (2010) 183-195.

[26] J.P. Ebejer, M.H. Charlton, P.W. Finn, Are the physicochemical properties of antibacterial compounds really different from other drugs?, J Cheminformatics, 8 (2016).

Journal Pre-proof

Journal Pre-proof

[27] D.G. Brown, T.L. May-Dracka, M.M. Gagnon, R. Tommasi, Trends and Exceptions of Physical Properties on Antibacterial Activity for Gram-Positive and Gram-Negative Pathogens, J Med Chem, 57 (2014) 10144-10161.

[28] S. Deresinski, Vancomycin in Combination with Other Antibiotics for the Treatment of Serious Methicillin-Resistant Staphylococcus aureus Infections, Clin Infect Dis, 49 (2009) 1072-1079.

[29] S.R. Singh, A.E. Bacon, D.C. Young, K.A. Couch, In vitro 24-hour time-kill studies of vancomycin and linezolid in combination versus methicillin-resistant Staphylococcus aureus, Antimicrob Agents Chemother, 53 (2009) 4495-4497.

[30] P. Yoong, V.J. Torres, The effects of Staphylococcus aureus leukotoxins on the host: cell lysis and beyond, Curr Opin Microbiol, 16 (2013) 63-69.

[31] M. Otto, Basis of Virulence in Community-Associated Methicillin-Resistant Staphylococcus aureus, Annu Rev Microbiol, 64 (2010) 143-162.

[32] A.H. Bartlett, K.G. Hulten, Staphylococcus aureus Pathogenesis Secretion Systems, Adhesins, and Invasins, Pediatr Infect Dis J, 29 (2010) 860-861.

[33] J.H. Melehani, D.B. James, A.L. DuMont, V.J. Torres, J.A. Duncan, Staphylococcus aureus leukocidin A/B (LukAB) kills human monocytes via host NLRP3 and ASC when extracellular, but not intracellular, PLoS Pathogens, 11 (2015) e1004970.

[34] T. Reyes-Robles, F. Alonzo, L. Kozhaya, D.B. Lacy, D. Unutmaz, V.J. Torres, Staphylococcus aureus Leukotoxin ED Targets the Chemokine Receptors CXCR1 and CXCR2 to Kill Leukocytes and Promote Infection, Cell Host Microbe, 14 (2013) 453-459.

Journal Pre-proof

[35] R.S. Flannagan, B. Heit, D.E. Heinrichs, Intracellular replication of Staphylococcus aureus in mature phagolysosomes in macrophages precedes host cell death, and bacterial escape and dissemination, Cell Microbiol, 18 (2016) 514-535.

[36] P. Vanderauwera, G. Prinz, G. Petrikkos, Activity of Intracellular Antibiotics, Infection, 19 (1991) S216-S223.

[37] R.M. Rakita, Intracellular activity, potential clinical uses of antibiotics, ASM News, 64 (1998) 570.

[38] T. Yamaoka, The bactericidal effects of anti-MRSA agents with rifampicin and sulfamethoxazole-trimethoprim against intracellular phagocytized MRSA, J Infect Chemother, 13 (2007) 141-146.

[39] R.G. Wunderink, J. Rello, S.K. Cammarata, R.V. Croos-Dabrera, M.H. Kollef, Linezolid vs vancomycin: analysis of two double-blind studies of patients with methicillin-resistant Staphylococcus aureus nosocomial pneumonia, Chest, 124 (2003) 1789-1797.

[40] A.D. Pimenta, L.D. Chiaradia-Delatorre, A. Mascarello, K.A. de Oliveira, P.C. Leal, R.A. Yunes, C.B.N.M. de Aguiar, C.I. Tasca, R.J. Nunes, A. Smania, Synthetic organic compounds with potential for bacterial biofilm inhibition, a path for the identification of compounds interfering with quorum sensing, Int J Antimicrob Ag, 42 (2013) 519-523.

[41] G.Z. Chen, L.R. Swem, D.L. Swem, D.L. Stauff, C.T. O'Loughlin, P.D. Jeffrey, B.L. Bassler, F.M. Hughson, A Strategy for Antagonizing Quorum Sensing, Mol Cell, 42 (2011) 199-209.

[42] A.S. Kwon, G.C. Park, S.Y. Ryu, D.H. Lim, D.Y. Lim, C.H. Choi, Y. Park, Y. Lim, Higher biofilm formation in multidrug-resistant clinical isolates of Staphylococcus aureus, Int J Antimicrob Ag, 32 (2008) 68-72.

Journal Pre-proof

Journal Pre-proof

[43] M.R. Kiedrowski, A.R. Horswill, New approaches for treating staphylococcal biofilm infections, Ann N Y Acad Sci, 1241 (2011) 104-121.

[44] L. Leonidou, C.A. Gogos, Catheter-related bloodstream infections: catheter management according to pathogen, Int J Antimicrob Ag, 36 (2010) S26-S32.

[45] P. Francois, J. Schrenzel, C. Stoerman-Chopard, H. Favre, M. Herrmann, T.J. Foster, D.P. Lew, P. Vaudaux, Identification of plasma proteins adsorbed on hemodialysis tubing that promote Staphylococcus aureus adhesion, J Lab Clin Med, 135 (2000) 32-42.

[46] A.L.S. Antunes, J.W. Bonfanti, L.R.R. Perez, C.C.F. Pinto, A.L.P.d. Freitas, A.J. Macedo, A.L. Barth, High vancomycin resistance among biofilms produced by Staphylococcus species isolated from central venous catheters, Mem Inst Oswaldo Cruz, 106 (2011) 51-55.

[47] N. Hoiby, O. Ciofu, H.K. Johansen, Z.J. Song, C. Moser, P.O. Jensen, S. Molin, M. Givskov, T. Tolker-Nielsen, T. Bjarnsholt, The clinical impact of bacterial biofilms, Int J Oral Sci, 3 (2011) 55-65.

[48] A. Kotb, N.S. Abutaleb, M. Hagras, A. Bayoumi, M.M. Moustafa, A. Ghiaty, M.N. Seleem, A.S. Mayhoub, tert-Butylphenylthiazoles with an oxadiazole linker: a novel orally bioavailable class of antibiotics exhibiting antibiofilm activity, RSC Adv, 9 (2019) 6770-6778.

[49] W.M. Dunne, Jr., E.O. Mason, Jr., S.L. Kaplan, Diffusion of rifampin and vancomycin through a Staphylococcus epidermidis biofilm, Antimicrob Agents Chemother, 37 (1993) 2522-2526.

[50] C. Clinical and Laboratory Standards Institute, Methods for dilution antimicrobial susceptibility tests for bacteria that grow aerobically, M7-A9. 9th ed. (2012).

Journal Pre-proof

[51] S. Thangamani, H. Mohammad, M.F.N. Abushahba, M.I. Hamed, T.J.P. Sobreira, V.E. Hedrick, L.N. Paul, M.N. Seleem, Exploring simvastatin, an antihyperlipidemic drug, as a potential topical antibacterial agent, Sci Rep-UK, 5 (2015).

Journal Pre-proof

Journal Pre-proof

1. Inserting a single N atom to lipophilic part of phenylthiazoles had a tremendous effect on PK profile.
2. The aqueous solubility increased by a factor of 160.
3. Compound **10** is an orally-available with C_{max} value higher than its MIC values.
4. Compound **10** is superior to vancomycin in term of the ability to disrupt mature biofilms.

Journal Pre-proof